

Voltammetric studies of the reactions of iron–sulphur clusters ([3Fe-4S] or [M3Fe-4S]) formed in *Pyrococcus furiosus* ferredoxin

Sarah E. J. FAWCETT*, David DAVIS*, Jacques L. BRETON†, Andrew J. THOMSON† and Fraser A. ARMSTRONG*¹

*Department of Chemistry, University of Oxford, South Parks Road, Oxford, OX1 3QR, U.K., and †Centre for Metalloprotein Spectroscopy and Biology, School of Chemical Sciences, University of East Anglia, Norwich NR4 7TJ, U.K.

Reactions of the [3Fe-4S] cluster and various metallated [M3Fe-4S] adducts co-ordinated in the ferredoxin from the hyperthermophile *Pyrococcus furiosus* have been studied by protein-film voltammetry, bulk-solution voltammetry, solution kinetics and magnetic CD (MCD). The [3Fe-4S] cluster exhibits two couples, [3Fe-4S]⁺⁰ and [3Fe-4S]^{0/2-}. Film voltammetry is possible over a wide pH range (2–8), revealing that the [3Fe-4S]⁺⁰ couple shows a complex pH dependence with $pK_{\text{red1}} = 2.8$, $pK_{\text{ox}} = 4.9$ and $pK_{\text{red2}} = 6.7$. From MCD, pK_{red1} corresponds with protonation of [3Fe-4S]⁰ to give a spectroscopically distinct species, as reported for ferredoxins from *Azotobacter* and *Sulfolobus*. The status of the disulphide/disulphydryl entity makes no significant difference to the data (given for the -S-S-

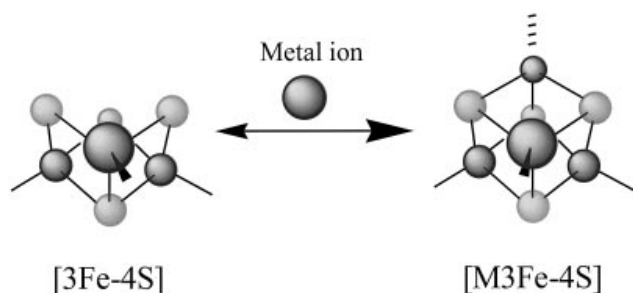
form). Formation of the hyper-reduced [3Fe-4S]²⁻ state is observed, requiring 3H⁺ for the overall 3e⁻ reduction of [3Fe-4S]⁺, the change therefore being electroneutral. By comparison with the ferredoxin from *Desulfovibrio africanus*, uptake of Fe(II) and other M(II) by [3Fe-4S]⁰ to give [M3Fe-4S] clusters is slow ($t_{1/2} > 10$ min at room temperature, slower still if the protein is adsorbed on the electrode), whereas reaction with Tl(I) to produce [Tl3Fe-4S] is very rapid ($t_{1/2} \ll 1$ s), suggesting that co-ordination of Tl does not require reorganization of the protein structure. Rates of formation of [3Fe-4S] from [M3Fe-4S] adducts increase sharply at high potentials, showing that metal release involves a labile ‘super-oxidized’ [M3Fe-4S]³⁺ state.

INTRODUCTION

Awareness and understanding of the biological, chemical and physical properties of iron–sulphur clusters are developing at a rapid rate, and it is becoming increasingly easy to identify trends and relationships in structure and reactivity [1]. An interesting aspect is the special ability of the cuboidal [3Fe-4S] cluster to function as a base, both in the Lewis and Brønsted sense.

First, there is a well-established tendency to co-ordinate a fourth metal (Scheme 1), resulting in the formation of [M3Fe-4S] cubanes (M = fourth metal atom) such as the familiar [4Fe-4S] cluster [2–20].

The [3Fe-4S] ↔ [M3Fe-4S] equilibrium provides the simplest



Scheme 1 Interconversion between cuboidal [3Fe-4S] and cubane [M3Fe-4S] clusters

example of interconversion between cluster types, and is observed, for example, in aconitase, where the 4Fe but not the 3Fe form is catalytically active [2,17,18]. Reversible transformation between [3Fe-4S] and [M3Fe-4S] clusters has been established for several small ferredoxins, and extended recently to a non-protein cuboidal [3Fe-4S] analogue [3–16,19,20]. Efforts are underway to determine the factors that govern this reactivity: electron-acceptor properties of M, cluster oxidation level, the availability of a suitable ligand for M and the absence of steric restrictions are each believed to be important [16,19,20].

Second, there is increasing evidence that the [3Fe-4S] cluster can bind one or more protons. Studies of the ferredoxins from *Azotobacter chroococcum* (Ac), *Azotobacter vinelandii* (Av) and *Sulfolobus acidocaldarius* (Sa) have revealed that the 1-electron-reduced-state [3Fe-4S]⁰ binds a single proton with pK values ranging from 7.8 to 5.8 [21–26]. The site of protonation has not yet been established [25]. The [3Fe-4S] cluster appears also able to support a ‘hyper-reduced’ state, [3Fe-4S]²⁻, associated with multiple proton uptake [27].

The biological significance of these reactivities is as yet unclear; however, addition and abstraction of metals are relevant to sensory systems responsive to cellular Fe or O₂ levels, while proton binding is implicated in the action of Fe-S enzymes that catalyse proton-coupled redox reactions, such as nitrogenase [28–30].

The ferredoxin from the hyperthermophile *Pyrococcus furiosus* (Pf) contains a single cluster which interconverts between [3Fe-4S] and [4Fe-4S] forms [7,8,31]. This cluster is co-ordinated by the atypical motif Cys-X₂-Asp-X₂-Cys-X_n-Cys, and there is spectroscopic evidence that the labile Fe is co-ordinated by the

Abbreviations used: DTNB, 5,5'-dithiobis(2-nitrobenzoic acid); MCD, magnetic CD; M, denoted as the fourth metal atom in iron–sulphur clusters; Ac Fd, Av Fd, Sa Fd, Pf Fd and Da Fd, ferredoxins from *Azotobacter chroococcum*, *Azotobacter vinelandii*, *Sulfolobus acidocaldarius*, *Pyrococcus furiosus* and *Desulfovibrio africanus*, respectively; SHE, standard hydrogen electrode.

¹ To whom correspondence should be addressed (e-mail fraser.armstrong@chem.ox.ac.uk).

aspartate [32,33]. A number of [M3Fe-4S] adducts have been characterized [9–11,19]. A similar motif co-ordinates the [3Fe-4S] cluster in the 7Fe ferredoxin (Fd III) from *Desulfovibrio africanus* (Da), which we have studied extensively and which also undergoes rapid, reversible transformations, although aspartate ligation has not been established unequivocally [12–16,34]. As far as can be deduced, aspartate ligation has several consequences: (i) it labilizes the cluster towards release of the O-bound Fe and binding of exogenous ligands [35–38]; (ii) reduced [4Fe-4S]⁺ clusters exist completely (Da Fd III) or partly (Pf Fd) in the unusual $S = 3/2$ spin state [7,12]; and (iii) the O-ligation (RCO₂⁻) does not markedly alter the reduction potential relative to conventional all-cysteine- (RS⁻) ligated clusters [34,39]. Although *P. furiosus* Fd is the simplest example, it contains additionally a disulphide bridge (in place of the second cluster), the influence of which is uncertain. Samples can be prepared which have the disulphide bridge intact (oxidized-Fd_A) or broken (reduced-Fd_B) [40].

Protein-film voltammetry is a relatively new method for studying redox-active sites in proteins [41,42]. Ideally, protein molecules are induced to adsorb on an innocuous electrode surface, at which they come under the control of the applied electrode potential, and redox-active sites become visible through their voltammetric signals. In the simplest case these are a pair of oxidation and reduction peaks centred at the formal reduction potential. The amount of material under observation is minuscule, yet reactions with trace levels of reactant in the contacting electrolyte can be detected and quantified by examination of changes in the positions and shapes of these signals. Transfer of the coated electrode between various solutions enables different reaction possibilities to be examined, including sensitivity to metal ions, ligands, substrates, and even extremes of pH or solvent that would cause denaturation on the timescale of a conventional titration. Rapid redox-coupled reactions can be detected with ease and quantified. It can also be ascertained whether, by comparison with studies carried out in solution, the film (electrode-bound) environment offers protection (resistance) to these reactions, i.e. does binding of the protein at a surface modify or restrict its chemistry?

We have now used protein-film voltammetry in conjunction with other methods to study the redox-coupled reactions of the [3Fe-4S] cluster in Pf Fd. First, we have sought to establish the complex pH-dependent redox chemistry of this cluster (so far examined only in 7Fe ferredoxins) in a protein that does not contain a second centre to complicate the spectroscopy. Second, to extend our knowledge of the relationships existing among thermodynamic properties, such as [M3Fe-4S] cluster stabilities and reduction potentials, we have compared the characteristics (equilibria and kinetics) of reversible metal-ion uptake and release with results of recent studies on Da Fd III [12–16]. The metals chosen (M = Fe, Zn, Cd, Tl) bind tightly to [3Fe-4S]⁰ in Da Fd III and the products have been spectroscopically characterized in Pf Fd itself [9–11,19]. Third, we have investigated the influence of cluster-extrinsic influences such as the presence or absence of the disulphide bridge and differences between bulk-solution and adsorbed-film environments.

EXPERIMENTAL

All electrochemical and spectroscopic operations were carried out using deionized water (Millipore, 18 MΩ·cm) and analytical grade reagents. Cells of *P. furiosus* (strain vc1) DSM 3638 were grown in a continuous culture in a glass lift bioreactor at 95 °C at the Centre for Applied Microbiology and Research, Porton Down, U.K. [43]. The ferredoxin was purified using a similar

method to that used by Aono et al. [31]. Concentrations were determined using $\epsilon_{390} = 17 \text{ mM}^{-1} \cdot \text{cm}^{-1}$ for the [4Fe-4S]²⁺ form, or $\epsilon_{408} = 18 \text{ mM}^{-1} \cdot \text{cm}^{-1}$ for the [3Fe-4S]⁺ form [7]. At 20 °C and under aerobic conditions, a mixture of the [3Fe-4S] and [4Fe-4S] ferredoxins was obtained that could be separated by FPLC (Pharmacia) using a Mono-Q HR 5/5 column. The protein, in 50 mM Tris, pH 7.6, was chromatographed with a 0–1.0 M NaCl gradient. The [4Fe-4S] form eluted first at 0.43 M NaCl followed by the [3Fe-4S] form at 0.45 M. As determined from the FPLC output (relative peak heights) and identified by UV-visible spectra, 60% of the aerobically purified protein was in the 4Fe form, with the remainder containing [3Fe-4S]. To convert the sample completely to the 3Fe form, a five-fold excess of K₃[Fe(CN)₆] was added and the protein was dialysed into 50 mM Tris (pH 7.6)/0.1 M NaCl/0.1 mM EGTA, using an Amicon 8MC unit equipped with a microvolume assembly and YM3 membrane.

Preparations of the 3Fe and 4Fe forms were made with the disulphide bridge either oxidized (Fd_A) or reduced (Fd_B) [40]. In all cases, the starting material was the aerobic, ferricyanide-oxidized form 3Fe Fd_A, with the disulphide bridge intact. To give 3Fe Fd_B, a sample of 3Fe Fd_A was reduced with a five-fold excess of dithiothreitol under anaerobic conditions for ≈ 72 hours and then exhaustively dialysed into 50 mM Hepes/0.1 M NaCl/0.1 mM EGTA, pH 7.4, to remove excess dithiothreitol. The 4Fe Fd_A and 4Fe Fd_B forms were prepared by adding dithionite (three-fold molar excess) and Fe²⁺ (five-fold molar excess) to the 3Fe Fd_A and 3Fe Fd_B forms (each typically 0.1 mM) respectively, and incubating for 15 min at room temperature. The status of the disulphide bridge was determined by titration with 5,5'-dithiobis(2-nitrobenzoic acid) (DTNB) [44]. The disulphide-bridge reduced (B) forms routinely gave 2.0 ± 0.1 free thiols/protein molecule, while the disulphide-bridge oxidized (A) forms produced no observable reaction, indicating the absence of free thiols. For the pH-dependence study carried out on the adsorbed films, a 20 mM mixed-buffer system was used, consisting of 5 mM in each of acetate, Mes, Hepes and Taps, with 0.1 M NaCl as supporting electrolyte. Solutions were adjusted to the required pH with either NaOH or HCl. For metal-ion uptake and release experiments, the cell buffer was either 20 mM mixed buffer or 50 mM Tris (pH 7.0) with 0.1 M NaNO₃ or 0.1 M acetate, pH 6.8, for studies with Tl. Metal-ion solutions were added as required from concentrated stocks: Fe²⁺ [(NH₄)₂SO₄·FeSO₄·6H₂O], Cd²⁺ [Cd(NO₃)₂], Tl⁺ (TlOOC·CH₃) and Zn²⁺ [ZnSO₄·7H₂O or Zn(NO₃)₂·6H₂O]. Polymyxin sulphate (Sigma), as co-adsorbate, was added to the buffers to give a final concentration of 200 μg/ml. For bulk-solution electrochemistry, protein concentrations were typically 40–80 μM in 20 mM Hepes/0.1 M NaCl/0.1 mM EGTA, with 2 mM neomycin (Sigma) to promote and stabilize the electrochemical response [26]. Most experiments were carried out in a glove box (Belle Technology, Dorset, England) with O₂ < 2 ppm.

DC cyclic voltammetry was carried out with an Eco-Chemie Autolab electrochemical analyser equipped for staircase CV voltammetry but also featuring fast-scan generator (Scangen) and analogue-to-digital converter (ADC750) modules for obtaining fast analogue voltammetry where necessary [45]. For some experiments, an Ursar Instruments potentiostat was used with scans recorded on a Kipp and Zonen XY or YT recorder. For most voltammetry, all-glass cells were used; either a single-pot cell for bulk-solution voltammetry, or a multipot cell for protein-film experiments requiring different pH values, addition of metals or sequestering agents. The multipot cell consisted of four individual pots radially connected to a central reference compartment, each pot having a platinum counter electrode. In

most cases, the temperature was thermostatted at 0 °C to optimize stability. The reference was a saturated calomel electrode (SCE) held at 22 °C. Potentials were converted to the standard hydrogen electrode (SHE) by using $E(\text{SCE}) = +243 \text{ mV}$ [46]. The pyrolytic graphite edge (PGE) electrode (area approximately 0.18 cm^2) was prepared for protein application by polishing with an aqueous alumina slurry (Buehler Micropolish, $1.0 \mu\text{m}$) and sonicating extensively in water to remove traces of Al_2O_3 .

To prepare films, a $\approx 1 \mu\text{l}$ aliquot of ice-cold ferredoxin solution (typically $100 \mu\text{M}$ in 50 mM Tris, pH 7.6, 0.1 M NaCl with $200 \mu\text{g/ml}$ polymyxin as co-adsorbate) was applied to the surface of the electrode with a fine glass capillary tip. Voltammograms were scanned first in a pot containing buffer-electrolyte at pH 7.0 in order to establish a film, then the electrode was transferred to other pots containing different solutions. In this way it was possible to perform 'instantaneous dialysis' and measure the behaviour of the system even under extreme conditions of pH. Neomycin was also employed as a co-adsorbate, with no obvious observable differences to polymyxin except that films were less stable.

Cluster transformations in solution were monitored in the glove box using a cuvette placed in an optical cell block and linked via fibre optics to a diode-array UV-visible spectrometer (Hi-Tech Scientific, Salisbury, U.K.). For magnetic CD (MCD), samples of 3Fe Fd_A ($300\text{--}500 \mu\text{M}$) in mixed buffer consisting of 40 mM in each of acetate, Mes, Hepes, 0.4 mM EDTA and pH 7.8, were reduced with excess sodium dithionite before adding glycerol (to 50% v/v) and adjusting the pH to the desired value using HCl. Samples were then divided into two, half being placed in a 1 mm pathlength MCD cell and the other half in an EPR tube. Low-temperature MCD was conducted using a Jasco J-500D dichrograph and an Oxford Instruments split-coil superconducting magnet SM4. Procedures for obtaining MCD spectra have been described elsewhere [47]. EPR spectroscopy was performed on an X-band Bruker ER200-D SRC spectrometer equipped with an Oxford Instruments ESR-900 helium flow cryostat and a TE102 cavity.

RESULTS

Voltammograms

Two methods were employed, film and bulk voltammetry, and the results were compared. Figure 1 shows film voltammograms of the two major FPLC fractions, measured at pH 7.0, 0 °C. From their UV-visible spectra, fraction 1 ($\lambda_{\text{max}} = 390 \text{ nm}$) and fraction 2 ($\lambda_{\text{max}} = 408 \text{ nm}$) comprise the $[4\text{Fe-4S}]$ and $[3\text{Fe-4S}]$ forms, respectively [7,31,39]. Both these samples had the disulphide bridge oxidized, as determined from DTNB titrations [44]. The $[4\text{Fe-4S}]_A$ form shows a single signal (pair of oxidation and reduction waves) at $E'_0 = -428 \text{ mV}$, whereas the $[3\text{Fe-4S}]_A$ form shows the characteristic voltammetric pattern observed for other proteins containing the $[3\text{Fe-4S}]$ cluster, i.e. a signal at higher potential (A') and a narrow but more intense signal at lower potential (C') [27]. For labelling purposes, we continue the notation adopted previously for *D. africanus* 7Fe Fd, the superscript indicating protein film measurement. Integration of the areas under signals A' and C' gave C'/A' ratios of 2.0 ± 0.3 for all samples examined. From our recent studies on $[3\text{Fe-4S}]$ clusters in several proteins, signal A' , with a reduction potential $E'_0 = -150 \text{ mV}$ at pH 7.0, is assigned to the redox couple $[3\text{Fe-4S}]^{+/0}$, and signal C' , $E'_0 = -695 \text{ mV}$ at pH 7.0, is assigned to the novel two-electron transformation $[3\text{Fe-4S}]^{0/2-}$ [27]. In accordance with previous notation, the single signal from the $[4\text{Fe-4S}]$ form is denoted D' , since it corresponds to a transformable $[M3\text{Fe-4S}]^{2+/+}$ cluster. All the peaks observed for 3Fe and 4Fe

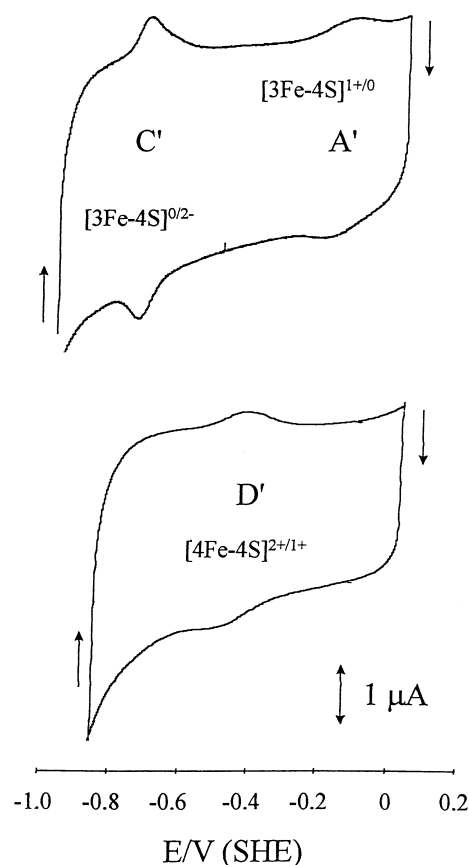


Figure 1 Film voltammograms of $[3\text{Fe-4S}]_A$ and $[4\text{Fe-4S}]_A$ forms of Pf Fd

Conditions: pH 7.0, 20 mM mixed buffer/ 0.1 M NaCl/ 0.1 mM EGTA, with polymyxin as co-adsorbate. Temperature 0 °C, scan rate $50 \text{ mV}\cdot\text{s}^{-1}$. Arrows indicate direction of cycling.

forms were consistently broader than we have observed for other ferredoxins, even at slowest scan rates, suggesting greater heterogeneity among molecules in the film. Experiments with samples in which the disulphide bridge was reduced gave similar results: for $[3\text{Fe-4S}]_B$, also at pH 7.0, we obtained; for signal A' , $E'_0 = -159 \text{ mV}$; for signal C' , $E'_0 = -714 \text{ mV}$. The $[4\text{Fe-4S}]_B$ form showed $E'_0 = -428 \text{ mV}$.

Bulk voltammetry was carried out with each form of the protein at pH 7.0, 0 °C. Some results are shown in Figure 2. Reduction potentials for the $[3\text{Fe-4S}]^{+/0}$ cluster are -215 and $-219 \pm 5 \text{ mV}$ respectively for $[3\text{Fe-4S}]_A$ and $[3\text{Fe-4S}]_B$ forms, essentially identical to the value reported by Smith et al. using differential-pulse voltammetry [48]. The reduction potentials for the $[4\text{Fe-4S}]_A$ or $[4\text{Fe-4S}]_B$ clusters in solution are -361 and $-365 \pm 5 \text{ mV}$. Thus, the bulk-solution reduction potentials deviate in opposite directions from values measured for the protein film. In each case, peak currents were proportional to the square root of scan rate (up to $20 \text{ mV}\cdot\text{s}^{-1}$) as expected for freely diffusing species. The low-potential couple in the potential region expected for $[3\text{Fe-4S}]^{0/2-}$ (i.e. corresponding to signal C' for the film) appeared only at very slow scan rates ($2 \text{ mV}\cdot\text{s}^{-1}$). As evident from the attenuated oxidation wave and disappearance on continued cycling, the complex proton-coupled redox chemistry, observed so readily for *S. acidocaldarius* ferredoxin, depends critically upon the state of the electrode interface, at which molecules must interact transiently. Evidently, these coupled

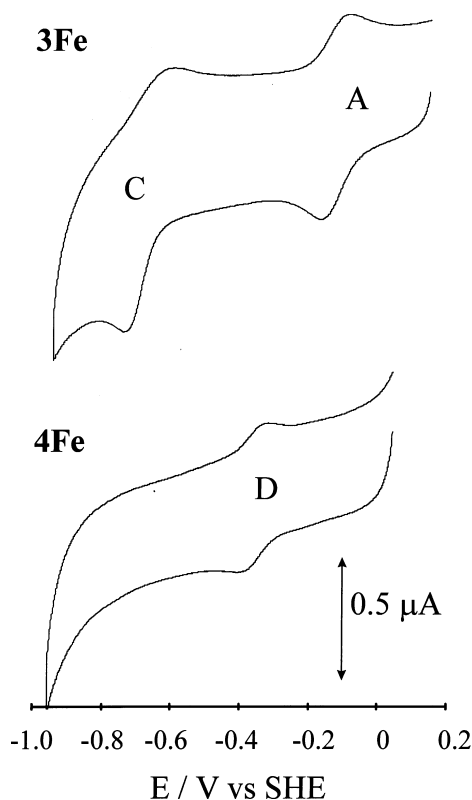


Figure 2 Bulk-solution voltammograms of $[3\text{Fe-4S}]_A$ ($42 \mu\text{M}$) and $[4\text{Fe-4S}]_A$ ($40 \mu\text{M}$) forms of Pf Fd

Conditions: pH 7.4, 20 mM Hepes/0.1M NaCl/0.1 mM EGTA/2 mM neomycin. Temperature 0°C , scan rate $2 \text{ mV} \cdot \text{s}^{-1}$.

reactions are facilitated when the protein is bound to the electrode [27].

pH dependence of reduction potentials

The pH dependencies of the reduction potentials were investigated by transferring the protein-coated electrode between solutions of various pHs. Even at pH 1.7 it was possible to achieve sufficiently stable films to make reliable measurements, and a sizeable data set was easily obtained. Graphs of reduction potentials as a function of pH are shown in Figure 3. Both $[3\text{Fe-4S}]_A$ and $[3\text{Fe-4S}]_B$ forms were investigated, and as can be seen, the two give essentially identical results. Both the A' and the C' couples show a complex pH dependence, whereas the D' couple is pH-independent. Considering A' first, there is clearly a region corresponding to protonation of the reduced form, but it is not possible to fit the curve to a simple scheme involving a single pK. For example, there is obviously a $\text{p}K_{\text{red}}$ at approximately pH 7, but the slope of the best straight line extending to the acid region is much less than predicted for a $1 \text{ H}^+ / 1 \text{ e}^-$ reaction. The best fit to the data for couple A' was obtained using Equation 1 [49]:

$$E'_0 = E'_{0\text{alk}} + \frac{RT}{nF} \ln \left[\frac{(a_{\text{H}^+})^2 + (a_{\text{H}^+})K_{\text{red1}} + K_{\text{red1}}K_{\text{red2}}}{(a_{\text{H}^+}) + K_{\text{ox}}} \right] \quad (1)$$

$E'_{0\text{alk}}$ is the reduction potential in the limit of high pH, a_{H^+} is the H^+ activity, n is the number of electrons transferred, and K_{red2} , K_{ox} and K_{red1} are successive H^+ -dissociation constants of reduced and oxidized species, appearing as the pH is decreased. Values

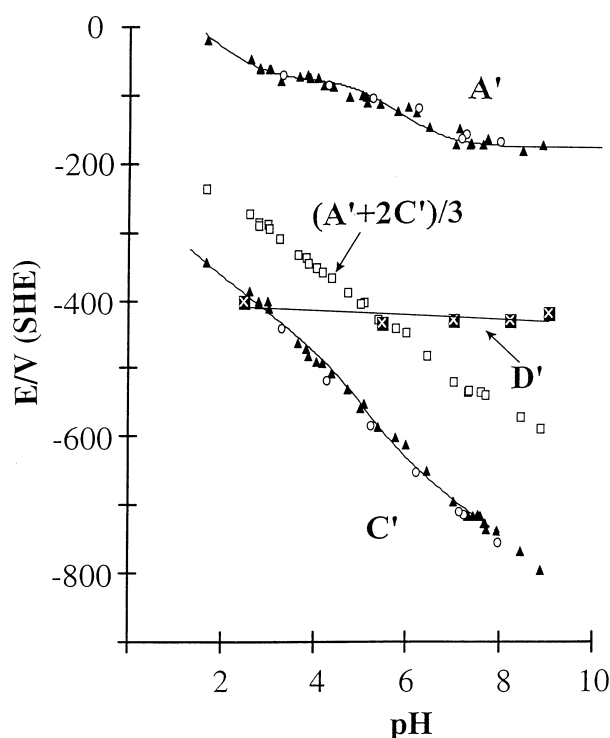


Figure 3 pH dependencies of couples A' and C' for different forms of Pf Fd

▲, $[3\text{Fe-4S}]_A$; ○, $[3\text{Fe-4S}]_B$ forms; □, weighted averages of A' and C' couples to give overall number of protons per electron for the three-electron reduction of $[3\text{Fe-4S}]^+$; ✕ are for the $[4\text{Fe-4S}]_A$ form (couple D').

obtained were: $\text{p}K_{\text{red1}} = 2.8$, $\text{p}K_{\text{ox}} = 4.9$ and $\text{p}K_{\text{red2}} = 6.7$. The corresponding line obtained for couple C' appears to mirror that for couple A', with the steeper portions coinciding approximately with the shallower sections of the couple A' line and vice versa. Data above pH 8 were less reliable because the peak size and reversibility were diminished. The overall proton uptake for the A' and C' couples was estimated as reported previously for the 7Fe ferredoxins from *D. africanus*, *S. acidocaldarius* and *A. vinelandii*, by averaging the nE'_0 values of A' and C' [27]. The resulting data produce a reasonably straight line between pH 2 and 8, with slope -51.0 mV/pH unit. The net ratio based on H^+/e^- is thus close to 1.0 (theoretical slope at $0^\circ\text{C} = -54.2 \text{ mV}$) showing, as found for other proteins, that the overall three-electron reduction of the $[3\text{Fe-4S}]^+$ cluster is accompanied by the uptake of 3H^+ (see Discussion).

MCD spectroscopy

The MCD spectra of the dithionite-reduced Pf Fd $[3\text{Fe-4S}]^0$ cluster were recorded in the pH range 1.0–8.25. Partial cluster loss occurred at the more acidic pH values, resulting in some uncertainty in the final concentration, and therefore in the final calculated intensity of the spectra. To allow for this, the samples were reoxidized after the MCD spectra had been recorded, and the final cluster concentration was re-determined by UV-visible spectroscopy. At least 50% of the clusters were still present after 15 min incubation at pH 1.0, thus confirming the extreme resistance of Pf Fd under acidic conditions.

Figure 4 shows MCD spectra of $[3\text{Fe-4S}]^0$ Pf Fd prepared at various pH values. The spectrum at pH 8.25 is essentially identical

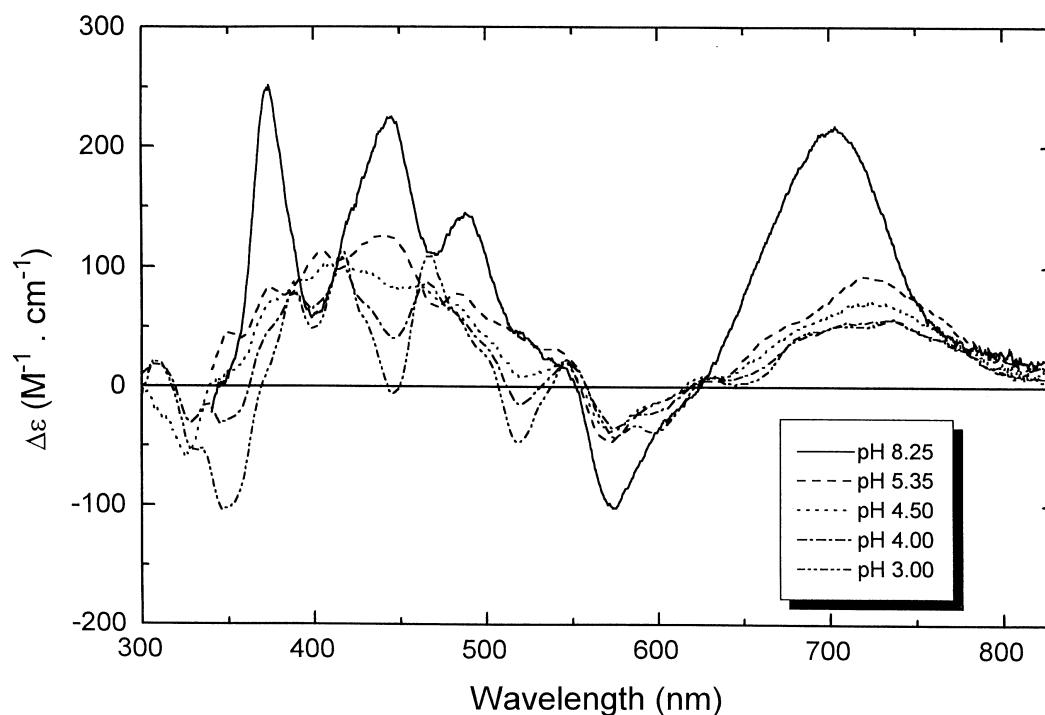


Figure 4 Low-temperature MCD spectra of *P. furiosus* [3Fe-4S]⁰ ferredoxin at various pH values

Ferredoxin concentrations are 150–200 μM in 50% (v/v) glycerol/water, containing 40 mM acetate and 0.4 mM EDTA. The spectra were measured at a temperature of 1.6 K and 5 Tesla, pathlength 1 mm.

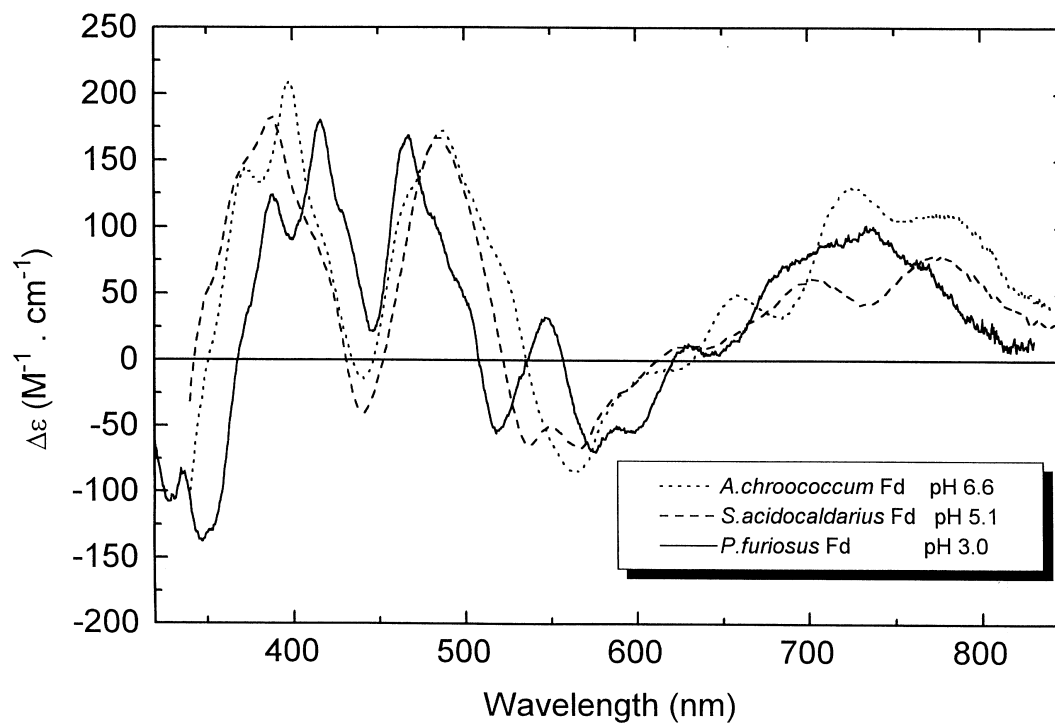


Figure 5 Comparison of the low-temperature MCD spectrum of the acid form of *P. furiosus* [3Fe-4S]⁰ ferredoxin with Ac Fd and Sa Fd

Spectra were measured at 4.2 K and 5 Tesla. The spectrum of Pf Fd has been multiplied by 2.0 to normalize the comparison with the other two spectra. (Sa Fd spectrum was taken from [26], Ac Fd spectrum from [21].)

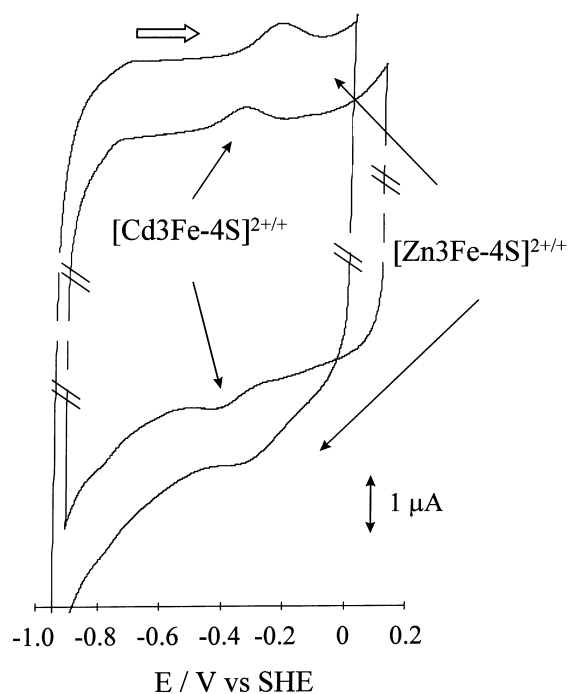


Figure 6 Film voltammograms of $[\text{Zn3Fe-4S}]_A$ and $[\text{Cd3Fe-4S}]_A$ forms of Pf Fd

Conditions: pH 7.0, 20 mM mixed buffer/0.1 M NaNO_3 . Temperature 0°C , scan rate $50 \text{ mV} \cdot \text{s}^{-1}$. The Cd adduct was prepared by poisoning a film of $[\text{3Fe-4S}]_A$ at -540 mV for 60 min. The Zn adduct was prepared by adding excess Zn^{2+} and excess sodium dithionite to a 0.1 mM solution of $[\text{3Fe-4S}]_A$ protein in bulk solution. Open arrow indicates direction of cycling.

to that reported by Conover et al. [7,19] and is characteristic of the $[\text{3Fe-4S}]^0$ cluster, having an $S = 2$ ground spin state with negative axial zero-field splitting [7,19,50]. It is very intense ($\Delta\epsilon_{\text{max}} \approx 250\text{--}300 \text{ M}^{-1} \cdot \text{cm}^{-1}$ at 1.6 K and 5 Tesla) with characteristic positive peaks around 370 nm, 445 nm and 700 nm, and a crossover at 550 nm. The EPR spectrum of the sample at low field showed only a broad trough ($g = '12'$ signal). The MCD spectrum undergoes a continuous series of changes as the pH is lowered, and at pH 3.0 the pattern of transitions is similar to the 'acid form' observed for other ferredoxins containing a protonated 3Fe cluster. Shown in Figure 5 are spectra for Ac Fd ($\text{p}K_{\text{red}} = 7.8$, [21,22]) and Sa Fd ($\text{p}K_{\text{red}} = 5.8$, [26]) while Av ferredoxin I ($\text{p}K_{\text{red}} = 7.8$, results not shown, [23]) is identical to Ac Fd. Another spectrum of Pf Fd (results not shown) was recorded at pH 1.0 and although this sample suffered extensive cluster destruction, the characteristic peak-to-trough distance (400–450 nm) was similar to that of the pH 3.0 sample. Thus the $\text{p}K$ for protonation of the reduced $[\text{3Fe-4S}]^0$ cluster of Pf Fd in bulk solution lies in the region of 3–4, and probably coincides with $\text{p}K_{\text{red1}}$ as determined by protein-film voltammetry, although note that comparisons between samples at 4.2 K in glycerol/buffer solution and protein films are difficult to make. The spectrum divides into two parts, with two sets of positive MCD bands ($\Delta\epsilon_{\text{max}} \approx 200 \text{ M}^{-1} \cdot \text{cm}^{-1}$ at 1.6 K and 5 Tesla) separated by a trough at 450 nm in the 300–550 nm region, and less-intense transitions at lower energy (550–850 nm). Comparisons of the spectra of the three ferredoxins in this region show that, upon protonation of the cluster, the intense 710 nm band splits into several less-intense constituents with positive signs. There is

Table 1 Comparisons of reduction potentials (mV), film versus bulk, disulphide bridge oxidized versus reduced, for $[\text{3Fe-4S}]$ and $[\text{M3Fe-4S}]$ clusters in Pf Fd

	Disulphide bridge oxidized (Fd_A)		Disulphide bridge reduced (Fd_B)	
	Film	Bulk	Film	Bulk
$[\text{3Fe-4S}]$	–150	–215	–159	–219
$[\text{Fe3Fe-4S}]$	–428	–361	–428	–365
$[\text{Zn3Fe-4S}]$	–262		–261	
$[\text{Cd3Fe-4S}]$	–359		–353	

some spectral variability among the different ferredoxins: the Pf Fd spectrum is about half as intense as those of the other two ferredoxins, although this may be due to the difficulty of determining the cluster concentration at the very acid pH values required for the experiment.

Metal uptake

First, samples of $[\text{M3Fe-4S}]$ Pf Fd with various M were obtained using a method similar to that described by Johnson and co-workers [11,19]. All operations were carried out in a glove box. An anaerobic solution of the 3Fe ferredoxin (either Fd_A or Fd_B ; $100 \mu\text{M}$) was placed in an Eppendorf tube together with sodium dithionite (0.4 mM) and an excess of the metal ion, and stirred for 15 min (25°C). The products were then examined voltammetrically by applying a small amount of protein to the electrode and scanning the film in pH 7.0 buffer-electrolyte. (Further purification was unnecessary since excess dithionite, metal ions etc. are released and diluted immediately into the bulk solution.) Film voltammograms of the products are shown in Figure 6. In each case signals A' and C' are replaced by a single new signal D' with reduction potentials depending on M. Samples of the Cd adduct had to be used within 2 h since excess Cd resulted in rapid loss of protein signals. We assign signal D' to the respective $[\text{M3Fe-4S}]^{2+/+}$ couples, based upon the agreement with data obtained for the isolated $[\text{4Fe-4S}]$ form and product characterization by Johnson and co-workers [11,19]. Reduction potentials of the transformation products of Fd_A and Fd_B are shown in Table 1.

Previous studies of Da Fd III showed that formation of $[\text{M3Fe-4S}]$ adducts could be conveniently executed and observed by the protein-film method [13–16,41,42]. A simple test for metal uptake involves cycling a film of the $[\text{3Fe-4S}]$ form of the protein in buffer-electrolyte containing different metal ions. Incorporation of M results in signals A' and C' disappearing and being replaced by a single signal D' (due to $[\text{M3Fe-4S}]^{+/0}$). The oxidation-level dependence of transformations is readily ascertained by holding the electrode potential at particular values, then cycling rapidly to view the products that have formed [13,16]. However, with Pf Fd we found that long periods were required to observe any transformations with Fe, Zn or Cd. For Zn and Cd, typical times required to achieve voltammograms similar to those shown in Figure 6 were of the order of 60 min. For Fe, no reaction at all was observed within this time, so experiments were performed at 25°C . At this temperature, the films are less stable but it was nonetheless possible to determine that approximately 50% conversion to $[\text{4Fe-4S}]$ had occurred after 60 min.

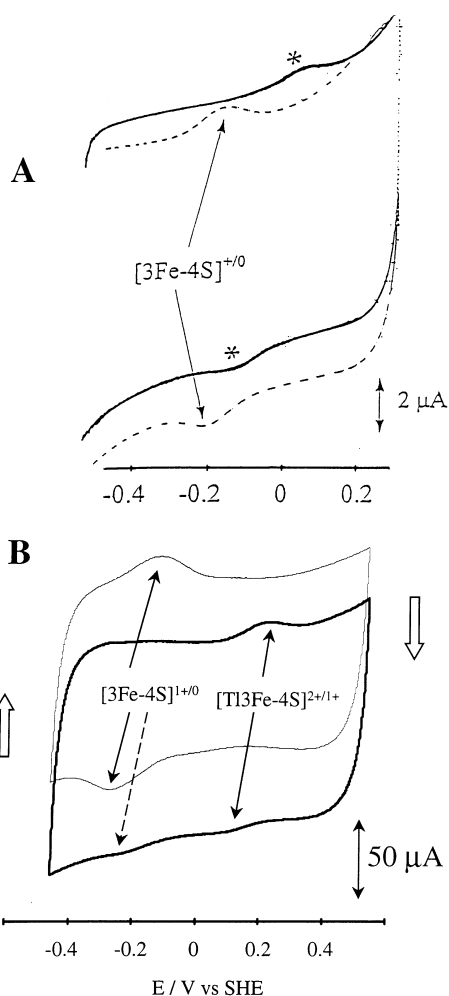
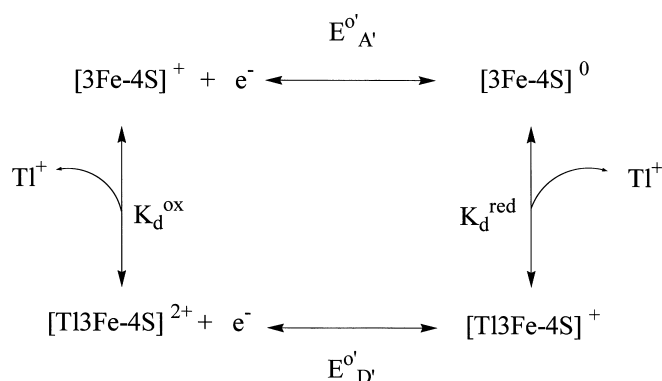


Figure 7 Film voltammetry of $[3\text{Fe-4S}]_A$ Pf Fd in the presence of Tl^+ (1 mM)

Temperature 0°C , pH 6.8, 0.1 M acetate/1 mM Tl^+ . (A) Scan rate $20\text{ mV}\cdot\text{s}^{-1}$. (B) Scan rate $30\text{ V}\cdot\text{s}^{-1}$. In both cases, the voltammetry of $[3\text{Fe-4S}]^{+/0}$ in the absence of Tl^+ is shown for comparison at the same scan rate (in faint or broken line).

By contrast, a very rapid and reversible reaction is observed with Tl^+ , producing $[\text{Tl3Fe-4S}]^{2+/+}$ [10]. Only Fd_A was studied, and results are shown in Figure 7. At slow scan rates (i.e. $\approx 10\text{ mV}\cdot\text{s}^{-1}$), voltammograms obtained for Pf Fd films contacting Tl^+ solutions show that signal A' moves to higher potential (Figure 7A), with the shift depending on Tl^+ concentration. It was not possible to observe the behaviour of signal C' due to Tl metal deposition at negative potentials. Significant changes occur as the scan rate is increased. Above $0.5\text{ V}\cdot\text{s}^{-1}$ the peaks shift back to the position observed in the absence of Tl^+ , and a second oxidation peak begins to appear at high potential. Figure 7(B) shows the voltammetry observed at $30\text{ V}\cdot\text{s}^{-1}$, from which it can be seen that the high-potential peak is now accompanied by a corresponding reduction wave, i.e. a second redox couple is becoming trapped out. As shown in Scheme 2, these results are interpreted in terms of rapid equilibria involving Tl^+ binding to both $[3\text{Fe-4S}]^+$ and $[3\text{Fe-4S}]^0$ forms [14].

Figure 8 shows that the data obtained at slow scan rates fit on a sigmoidal-shaped curve: the lower limit is the reduction potential of $[3\text{Fe-4S}]^{+/0}$, while the upper limit ($152 \pm 5\text{ mV}$) is the



Scheme 2 Coupled equilibria involving electron transfers and binding of Tl^+ to oxidized (+) and reduced (0) levels of the $[3\text{Fe-4S}]$ cluster

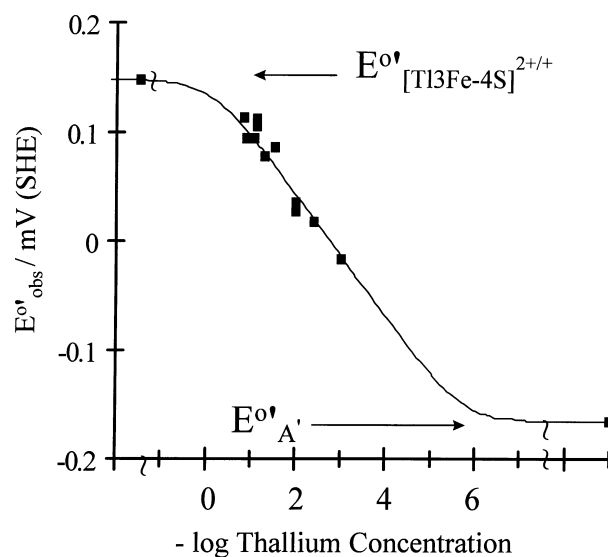


Figure 8 Variation of the reduction potential of $[3\text{Fe-4S}]$ Pf Fd with Tl^+ concentration

Conditions: pH 6.8, 0.1 M acetate, temperature 7°C . The upper and lower limits are, respectively, reduction potentials of the $[\text{Tl3Fe-4S}]^{2+/+}$ couple trapped at $30\text{ V}\cdot\text{s}^{-1}$, and $[3\text{Fe-4S}]^{+/0}$ cluster recorded in the absence of Tl^+ .

reduction potential of $[\text{Tl3Fe-4S}]^{2+/+}$ (E'_{D}), as measured at $30\text{ V}\cdot\text{s}^{-1}$, which is sufficiently fast to trap the weakly bound oxidized form. It is important to note that the technique enables this reduction potential to be measured without requiring an impractically high concentration of Tl^+_{aq} . A good fit to Equation 2 was obtained:

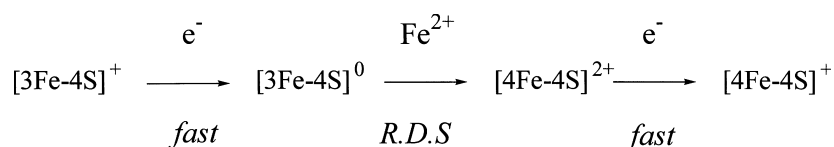
$$E'_{\text{obs}} = E'_{\text{OA}} + (2.303RT/F) \log\left\{ \frac{(1 + [\text{Tl}^+]/K_d^{\text{red}})}{(1 + [\text{Tl}^+]/K_d^{\text{ox}})} \right\} \quad (2)$$

using the value of E'_{D} obtained at high scan rate to define K_d^{ox} according to Equation 3:

$$E'_{\text{D}} = E'_{\text{OA}} + (2.303RT/F) \log(K_d^{\text{ox}}/K_d^{\text{red}}) \quad (3)$$

K_d^{ox} and K_d^{red} were calculated as 740 mM and 1.9 μM , respectively.

For the slower-reacting divalent metals it was possible to study the metal-uptake kinetics independently in bulk solution by



Scheme 3 Reaction sequence used to measure the rate of binding of Fe(II) to the [3Fe-4S]⁰ cluster

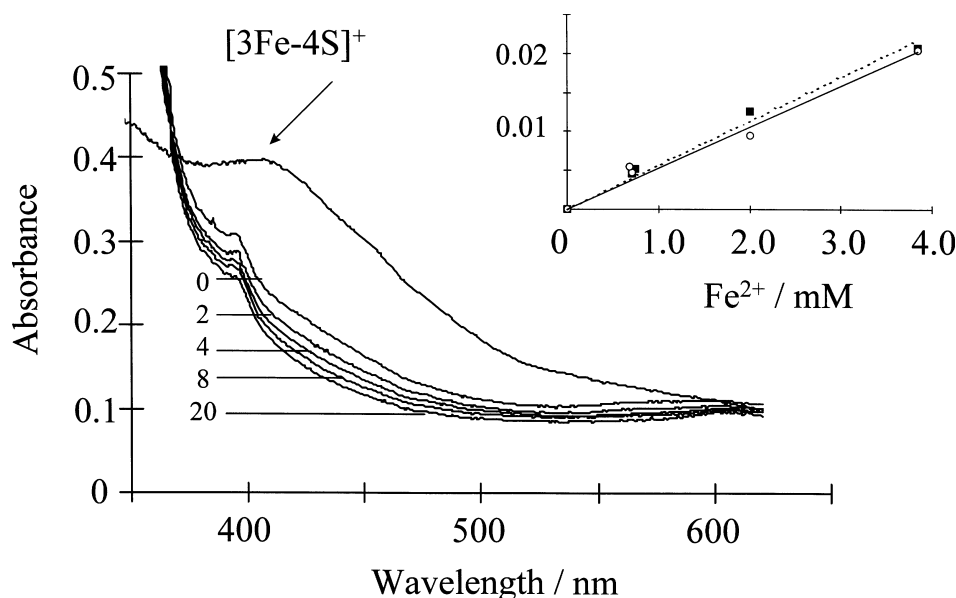


Figure 9 UV-visible spectra monitoring the uptake of Fe(II) into the [3Fe-4S]⁰ cluster of Pf Fd

Results shown are for the [3Fe-4S]_B cluster. The first two spectra correspond respectively to the [3Fe-4S]⁺ cluster and the product of reduction by sodium dithionite in the presence of methyl viologen (0 min). Subsequent spectra were recorded at intervals (times in min indicated) after addition of Fe(II). Temperature 25 °C. Inset, variation of measured first-order rate constants (ordinate = $k_{\text{obs}}/\text{s}^{-1}$) with Fe(II) concentration.

spectrophotometry, utilizing the ability of the immediate product [M3Fe-4S]²⁺ to undergo further reduction to [M3Fe-4S]⁺. We therefore undertook a study of Fe(II) uptake as depicted in Scheme 3.

Provided reduction of the [4Fe-4S]²⁺ product is fast, the kinetics are controlled by the rate of metal ion uptake [51]. Experiments were carried out to compare the reactivities of Fd_A and Fd_B with the very slow reactions observed for the corresponding protein film experiments.

The UV-visible spectra of the [3Fe-4S] forms of Fd_A or Fd_B were recorded before reduction with a 25-fold excess of dithionite in the presence of 1 μM methyl viologen as mediator. The spectrum was remeasured to ensure reduction was complete, and then a known quantity of Fe(II) was added and spectra were recorded at regular time intervals until there was no further absorbance change. These experiments were carried out at 25 °C for three different Fe(II) concentrations, and a typical result is shown in Figure 9. In each case, plots of log Δ*A* against time were linear to at least two half lives, giving pseudo-first-order rate constants k_{obs} . Reactions were first order in [Fe(II)] according to Equation 4:

$$\text{Rate} = k_{\text{uptake}}[3\text{Fe-4S}][\text{Fe(II)}] \quad (4)$$

Second-order rate constants k_{uptake} obtained for Fd_A and Fd_B were essentially identical, respective values being 5.28 M⁻¹·s⁻¹ and 5.23 M⁻¹·s⁻¹.

Metal release

Experiments to determine the electrode potentials critical for controlling metal-ion release from [M3Fe-4S] clusters were carried out as described previously for *D. africanus* 7Fe Fd [16]. Samples of Fd_A and Fd_B with transformed clusters [M3Fe-4S], M = Fe, Zn and Cd, were prepared chemically using dithionite. Samples were then adsorbed on to the electrode, and the potential was cycled between -900 mV and increasingly positive upper-switching potentials. Figure 10 shows the results obtained with Cd: the marked potential dependence of the formation of [3Fe-4S] is clearly observed.

To evaluate the effect of potential more closely and gauge relative rates of reaction, films were poised at different potentials for time intervals of 60 s, following which a cycle was recorded. In all cases, no formation of the [3Fe-4S] cluster was discernible at negative potentials (-757 or -457 mV), even after holding for 10 min with 0.1 mM EGTA in solution. Subjecting to more positive potentials produced contrasting results for the different clusters, although no additional couples attributable to reversible 'super-oxidation' processes were observed. Greatest lability was shown by the [Zn3Fe-4S] cluster; 50% release was recorded after 10 min at 43 mV and complete recovery of [3Fe-4S] was achieved after 10 min at 143 mV. The [Cd3Fe-4S] cluster is less reactive, with approximately 50% release after 10 min at 143 mV; however, release was virtually complete after 2 min at 243 mV. By

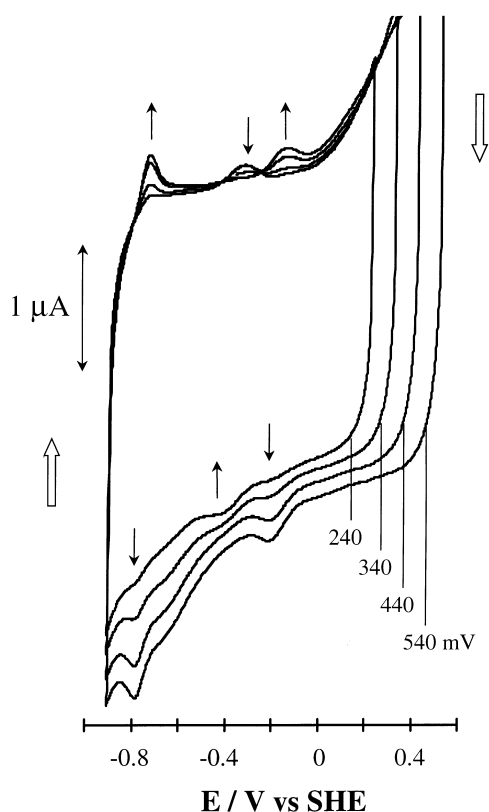


Figure 10 Film voltammetry showing release of Cd from the [Cd3Fe-4S] cluster of Pf Fd

The [Cd3Fe-4S] cluster was prepared from the [3Fe-4S]_A form by poisoning a film at -540 mV in the presence of Cd. A series of voltammograms (scan rate $50 \text{ mV} \cdot \text{s}^{-1}$) were then recorded at increasingly positive switching potentials after transfer to a pot containing 20 mM mixed buffer, pH 7.0, 0.1 M NaNO₃, with 0.1 mM EGTA. Temperature 0 °C. The broad reduction wave appearing at approximately -720 mV is an electrode-surface process induced by cycling to oxidizing potentials. Open arrows indicate direction of cycling.

contrast, the [Fe3Fe-4S] cluster is much more resistant to degradation; after 10 min at 443 mV the voltammogram was essentially unchanged, i.e. still that of the [Fe3Fe-4S] form with just a trace of [3Fe-4S]. In no cases were any significant differences observed between Fd_A and Fd_B forms.

DISCUSSION

pH dependence of reduction potentials

The [3Fe-4S] form exhibits complex pH-dependent redox chemistry, with reduction potentials that are insensitive to the presence of the disulphide bridge. First, and as established for other 3Fe-containing proteins (Av Fd I, Da Fd III and Sa Fd) the film voltammetry is dominated by the sharp two-electron signal at low potential [27]. Significantly, formation of the hyper-reduced state [3Fe-4S]²⁻, which has been partially characterized in *Sulfolobus* Fd, is now identified in a protein containing only a [3Fe-4S] cluster. In addition it was possible to observe this redox couple in molecules diffusing freely between the solution and the electrode interface, but only at very low scan rates. As discussed previously, the two-electron/multiple-proton redox reaction is dependent on complex coupled processes that require a prolonged residence time at the electrode [27]. Hence the appearance of the voltammetric wave is restricted to experiments with protein

films, except where the processes are clearly more facile (as with Sa Fd) or at extremely slow scan rates as found here for Pf Fd. The disappearance with continued slow cycling may reflect instability of the [3Fe-4S]²⁻ state in this ferredoxin.

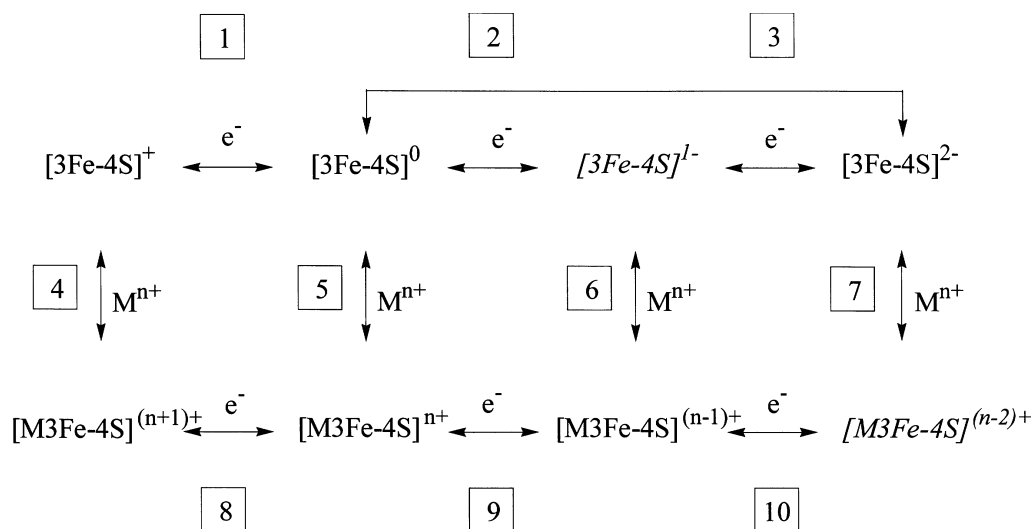
The pH dependence of the [3Fe-4S]⁺⁰ couple can be interpreted in part from the MCD results, which show that a complex series of changes occur, culminating, at pH < 3, in a form similar to that generated in other ferredoxins [21–26]. Protonation must now be considered to be a characteristic property of [3Fe-4S]⁰ centres, although there is a large variation in p*K* values, with the cluster in *Azotobacter* ferredoxins being particularly basic [22–24]. The observation that the [4Fe-4S] cluster in Fd_A or Fd_B shows little pH dependence of reduction potential suggests strongly the involvement of aspartate-14, which becomes ligated upon metal-ion addition. Reported p*K* values for aspartate in proteins cover a wide range, with 5.5 being quite usual [52]. However, the carboxylate p*K* will be sensitive to the oxidation level of the [3Fe-4S]⁺⁰ cluster due to the introduction of a nearby negative charge, and since invariably p*K*_{red} > p*K*_{ox}, we assign p*K*_{ox} = 4.9 and p*K*_{red} = 6.7 to deprotonations of aspartate-14 in oxidized and reduced forms respectively. Although these ionizations occur within the sequence of spectral changes in the MCD, and leave the p*K* at 2.8 as the formal value for [3Fe-4S]⁰ protonation, it is probable that the stepwise addition of two protons to the cluster region will involve anti-cooperative interactions between the aspartate and the cluster, thus giving rise to the complex drawn-out titration profile.

The pH dependence for the overall conversion of [3Fe-4S]⁺ to [3Fe-4S]²⁻, as judged from the average of the [3Fe-4S]⁺⁰ and [3Fe-4S]^{0/2-} couples, amounts to -51.0 mV/pH unit, which compares with values of -50.1 , -49.8 , and -51.4 mV/pH unit determined for Av Fd I, Sa Fd and Da Fd III respectively [27]. The net H⁺/e⁻ uptake ratio is thus close to 1.0, reinforcing an emerging consensus that reduction of the well-characterized oxidized [3Fe-4S]⁺ cluster to the enigmatic ‘hyper-reduced’ state [3Fe-4S]²⁻ requires net transfer of three protons from bulk solution. The corresponding electroneutrality of the overall reduction is probably responsible for the surprisingly good average straight line for the mirrored A’ and C’ pH dependencies. This is expected because the electrostatic influence of the state of ionization of a nearby residue (e.g. aspartate-14) on the reduction potential is quenched (compare with the A’ couple alone).

Cluster transformations

Transformations between the [3Fe-4S] and [M3Fe-4S] adducts can be discussed with reference to the framework shown in Scheme 4, in which species as yet undetected in this protein are indicated in italics [16]. M is either M(II) or M(I) (i.e. Tl). Several comparisons can be drawn with studies carried out on Da Fd III.

First, rates of metal uptake (reaction 5) measured under potential control in a film of Pf Fd are much slower than observed for Da Fd III [13,16]. Indeed, with M = Fe, reaction in Pf Fd at 25 °C was estimated to be only 50% complete after 60 min, compared with less than 1 min at 0 °C for Fd III under comparable Fe levels. Because of this sluggishness, equilibrium constants for reaction 5 could not be measured as they have been for Da Fd III. By contrast, uptake and release of Tl⁺ is very fast, with electrochemical equilibration occurring on voltammetric timescales just slightly longer than used for Da Fd III at a temperature of 0 °C. [14]. In the latter case, the system described by the Scheme 4 cycle, 1, 5, 8 and 4 is fully equilibrated for [Tl⁺_{aq}] < 5 μM at scan rates below $1 \text{ V} \cdot \text{s}^{-1}$, thereby indicating reaction rates close to diffusion control. With Pf Fd some hysteresis is noted at this scan rate, and by increasing to $30 \text{ V} \cdot \text{s}^{-1}$



Scheme 4 How different Fe-Scores ($[3\text{Fe-4S}]$ and $[M3\text{Fe-4S}]$) are interconnected by metal-ion binding and electron transfers

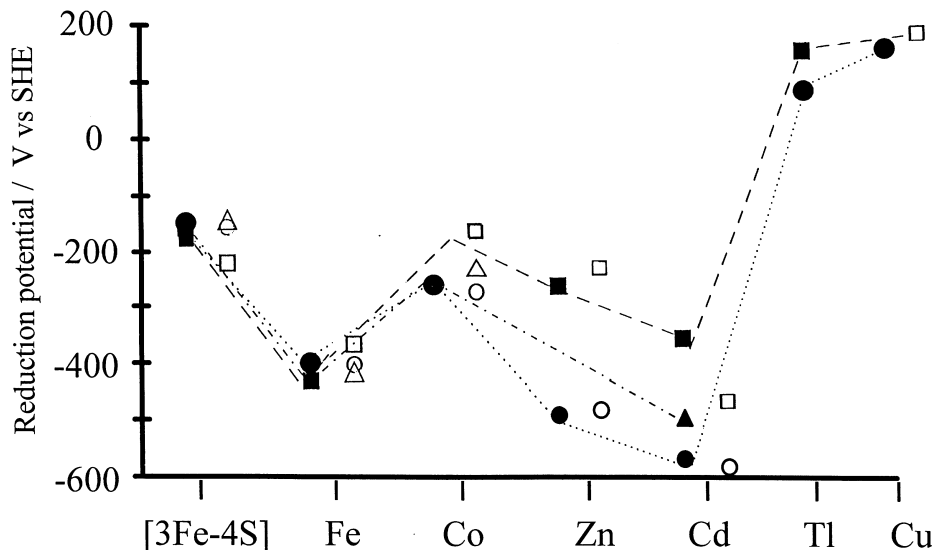


Figure 11 Comparisons of the reduction potentials of the $[3\text{Fe-4S}]$ clusters and various $[M3\text{Fe-4S}]$ adducts formed in ferredoxins from *P. furiosus* (■, □), *D. africanus* (●, ○) and *D. gigas* (▲, △)

Data taken from [16] and [19]. In most cases, pH = 7.0, temperatures were 0 °C to room temperature. Closed symbols displaced to left represent voltammetric values measured for protein films; open symbols displaced to right represent values for bulk-solution measurements (voltammetry or EPR-monitored potentiometry).

the oxidized adduct $[\text{Tl}3\text{Fe-4S}]^{2+}$ starts to be trapped out. The equilibrium constant for Tl^+ and $[3\text{Fe-4S}]^0$ (i.e. $K_d^{\text{red}} = 1.9 \mu\text{M}$) is similar to that for Da Fd III ($1.5 \mu\text{M}$) whereas binding to the oxidized cluster is weaker ($K_d^{\text{ox}} 0.74 \text{ M}$ versus 0.034 M) [14].

The spectrophotometric determinations of the rates of Fe(II) uptake at the $[3\text{Fe-4S}]^0$ cluster in solution clearly show: (i) that the protein is more reactive in solution than in the film, (ii) that the uptake follows simple second-order kinetics up to 4 mM Fe(II), and (iii) that the presence or absence of the disulphide bridge makes no difference to the rates. Film instability prevented experiments being performed at high temperatures where higher reactivity is expected. The situation with Tl is not so clear, since the equivalent solution experiment could not be performed. However, Johnson and co-workers have established that Tl, Fe,

Zn and Cd are each co-ordinated by the $[3\text{Fe-4S}]$ core [9–11,19]. Thus since Tl^+ still reacts so rapidly with $[3\text{Fe-4S}]^0$ we conclude that the slow rate of M(II) uptake is not due to the cluster domain being obscured in the protein film. The other explanation is that Tl^+ and the M(II) ions are not co-ordinated in the same way by the protein and make different demands on the mobility of residues. A likely possibility is that Tl^+ requires only the tri- μ_2 -sulphido face of the cluster, the co-ordination sphere being completed by weakly bound solvent molecules, thereby entirely overriding the activation requirements for positioning a protein ligand for co-ordination. This proposal is supported by the recent preparation of a Tl^+ adduct of the cuboidal $[3\text{Fe-4S}]$ analogue, where analysis of the isolated pure product $(\text{Et}_4\text{N})_2[\text{TlFe}_3\text{S}_4(\text{LS}_3)]$ reveals no additional ligand to

Tl [20]. It follows that rapid Tl⁺ exchange could provide a simple criterion for identifying exposed or readily accessible [3Fe-4S] clusters in proteins. For the much slower binding of M(II), the need to move residues to place aspartate-14 into a co-ordinating position would explain the difference in rates between solution and film, since certain modes of freedom may be restricted when the protein is bound to the graphite surface.

The potential dependence of metal-ion release provides strong evidence for the release of Fe, Zn and Cd via the 'super-oxidized' level equivalent to oxidized high-potential iron protein (HiPIP) and proceeding (Scheme 4) via pathways 8 → 4. The threshold potentials are well above that required to promote metal release from [M3Fe-4S]²⁺ by trapping the product as [3Fe-4S]⁺, i.e. utilizing pathways 5 → 1. Furthermore, the Fe, Zn and Cd adducts show different threshold potentials, with Fe requiring the most forcing conditions. However, in no case was a discrete signal observed at higher potential that could be attributable to a reversible redox couple. In a square-wave voltammetric study of aconitase [citrate (isocitrate) hydrolase] at a PGE electrode, Tong and Feinberg [18] reported a reduction potential of +100 mV (SHE) for the [4Fe-4S]^{3+/2+} couple, and its conversion to the [3Fe-4S]⁺ form was followed directly with EPR. A similar case has been reported for an active-site mutant of *Chromatium vinosum* HiPIP [53]. Much higher potentials are required to cause destruction of [4Fe-4S] clusters in *Clostridium pasteurianum* 8Fe ferredoxin [54]. Model studies also provide evidence that [4Fe-4S] clusters degrade to [3Fe-4S] via the 3+ level [55]. By contrast, for Da Fd III, rapid metal-ion release from [M3Fe-4S] is induced merely by applying a potential at which the [3Fe-4S] product is trapped in the 1+ level (thus identifying pathways 5 → 1 as a viable route) [16].

We have determined that divalent metal exchange in the [3Fe-4S]/[M3Fe-4S] cluster system occurs much faster for Da Fd III (typical reaction times at 0 °C are of the order of seconds) than for Pf Fd (several minutes at room temperature). Neither protein structures are known, but two possible contributing factors are evident from the amino-acid sequences that co-ordinate the [3Fe-4S] or [M3Fe-4S] cluster [33,34]:

Da Fd III **CTGDGEC** ----- **CE**

Pf Fd **CTGDAIC** ----- **CP**

Cluster-coordinating residues are shown in bold type. Greater mobility in the cluster region of Da Fd III ought to be favoured by the presence of glycine either side of the putative ligand aspartate, and from the unusual presence of glutamate instead of proline following the remote cysteine.

Reduction potentials

First, comparing reduction potentials measured for bulk solution with those measured for the film, we observe that the shifts observed for Pf Fd are much larger than we have observed for Da Fd III or in studies on Av Fd I [13,16,24]. The fact that shifts for different clusters run in opposite directions (for example, the film environment favours [3Fe-4S]⁰ (reduced) but [4Fe-4S]²⁺ (oxidized) states) is further evidence that binding of M(II) necessitates specific conformational changes, since this would lead naturally to variations in the energy of protein binding to the electrode. The binding of Cd is a particularly vivid example, since the value reported by Johnson and co-workers (−470 mV) for the free protein (measured by EPR titration) is much lower than our value of −359 mV [19]. We encountered difficulty measuring bulk voltammetry of the [Cd3Fe-4S] product because

of interference by the excess Cd²⁺ required to form the cluster in solution.

Finally, we consider the reduction potentials for [M3Fe-4S]^{2+/+} clusters generated in the three ferredoxins *Pf* Fd, *Da* Fd III and *Dg* Fd. Figure 11 displays data obtained by a variety of methods, in addition to which Holm and co-workers have measured reduction potentials for a number of non-protein analogues [20]. Apart from the larger discrepancy with Cd, the differences (EPR titration versus voltammetry, protein film versus bulk solution) are relatively small compared with the variations with different Ms. If an intrinsic factor, i.e. electron-withdrawing power, was the only determinant of reduction potential, then the same trend would be observed for all proteins. The intrinsic order is approximated most closely by the non-protein analogue data, for which Fe < Co < Ni < [3Fe-4S] < Cu < Tl serves as a good guide [20]. For the proteins, the consensual trends are Fe < Co < [3Fe-4S] < Tl and Cd < Zn. Departures from these orders must be attributed to protein structure. Scheme 4 shows that reduction potentials for reactions 8 (M = Tl, Cu) or 9 [M = M(II)] are related by thermodynamic cycles to the potentials for reactions 1 ([3Fe-4S]⁺⁰) or 2 ([3Fe-4S]^{0/-}), and the relative magnitudes of equilibrium constants; respectively, reactions 4 versus 5, and 5 versus 6 [16]. The latter will depend both on intrinsic effects and the nature and availability of non-cluster ligation. In addition, whereas the data show that the [3Fe-4S]⁺⁰ potentials (reaction 1) are similar for all three proteins, the same may not be true for [3Fe-4S]^{0/-} potentials, which we cannot measure.

In conclusion, our experiments on *Pf* Fd resolve and quantify some of the important emerging aspects of the ability of [3Fe-4S] clusters to bind protons and metal ions, the full biological implications of which remain to be established. Protonation of the one-electron reduced [3Fe-4S]⁺ cluster occurs to give a form spectroscopically similar to those generated in other proteins; however, the pK is much lower, being approximately 3. We have shown that two-electron reduction of [3Fe-4S]⁰ occurs as reported for several other proteins, and that formation of [3Fe-4S]²⁻ requires overall uptake of three protons relative to the fully oxidized form [3Fe-4S]⁺. These protonation equilibria and the extensive redox chemistry provide a striking contrast to the single-electron, non-protonic chemistry most typically associated with 2Fe and 4Fe clusters. We have compared rates of cluster transformations, identifying Tl interchange as a particularly facile process that may occur without protein reorganization and might therefore provide a diagnostic test for [3Fe-4S] clusters able to present a solvent-exposed face. For Fe, Zn and Cd, uptake reaction rates are much slower than observed for the ferredoxin from *D. africanus* and are sensitive to the external environment (free solution versus bound to electrode surface) but not to the presence or absence of the disulphide bridge. Release of M(II) is slow but is greatly accelerated at oxidizing potentials well in excess of those required to trap the [3Fe-4S]⁺ product, thereby revealing the participation of a labile super-oxidized state, most likely [M3Fe-4S]³⁺.

Note added in proof (received 7 September 1998)

During the time of submission of this article, a paper appeared by Adams and co-workers [Breraton, P. S., Verhagen, M. F. J. M., Zhou, Z. H. and Adams, M. W. W. (1998) *Biochemistry* **37**, 7351–7362] which included measurements of the pH dependence of reduction potentials of 3Fe and 4Fe clusters in *Pyrococcus furiosus* ferredoxin. The measurements made by these authors are in broad agreement with our own, although our analysis and interpretation differ in detail.

This research was supported by grants from the U.K. Engineering Physical Science Research Council (EPSRC, GR/J84809 to F.A.A.) and from the Biomolecular Sciences Panel of the EPSRC and the Biotechnology and Biological Sciences Research Council (to A.J.T.).

REFERENCES

- Beinert, H., Holm, R. H. and Münck, E. (1997) *Science* **277**, 653–659
- Kent, T. A., Dreyer, J.-L., Kennedy, M. C., Huynh, B. H., Emptage, M. H., Beinert, H. and Münck, E. (1982) *Proc. Natl. Acad. Sci. U.S.A.* **79**, 1096–1100
- Moura, J. J. G., Moura, I., Kent, T. A., Lipscomb, J. D., Huynh, B. H., LeGall, J., Xavier, A. V. and Münck, E. (1982) *J. Biol. Chem.* **257**, 6259–6267
- Moura, I., Moura, J. J. G., Münck, E., Papaefthymiou, V. and LeGall, J. (1986) *J. Am. Chem. Soc.* **108**, 349–351
- Surerus, K. K., Münck, E., Moura, I., Moura, J. J. G. and LeGall, J. (1987) *J. Am. Chem. Soc.* **109**, 3805–3806
- Moreno, C., Macedo, A. L., Moura, I., LeGall, J. and Moura, J. J. G. (1994) *J. Inorg. Biochem.* **53**, 219–234
- Conover, R. C., Kowal, T. J., Fu, W., Park, J.-B., Aono, S., Adams, M. W. W. and Johnson, M. K. (1990) *J. Biol. Chem.* **265**, 8533–8541
- Conover, R. C., Park, J.-B., Adams, M. W. W. and Johnson, M. K. (1990) *J. Am. Chem. Soc.* **112**, 4562–4564
- Srivastava, K. K. P., Surerus, K. K., Conover, R. C., Johnson, M. K., Park, J.-B., Adams, M. W. W. and Münck, E. (1993) *Inorg. Chem.* **32**, 927–936
- Fu, W., Telsler, J., Hoffman, B. M., Smith, E. T., Adams, M. W. W., Finnegan, M. G., Conover, R. C. and Johnson, M. K. (1994) *J. Am. Chem. Soc.* **116**, 5722–5729
- Finnegan, M. G., Conover, R. C., Park, J.-B., Zhou, Z. H., Adams, M. W. W. and Johnson, M. K. (1995) *Inorg. Chem.* **34**, 5358–5369
- George, S. J., Armstrong, F. A., Hatchikian, E. C. and Thomson, A. J. (1989) *Biochem. J.* **264**, 275–284
- Butt, J. N., Armstrong, F. A., Breton, J., George, S. J., Thomson, A. J. and Hatchikian, E. C. (1991) *J. Am. Chem. Soc.* **113**, 6663–6670
- Butt, J. N., Sucheta, A., Armstrong, F. A., Breton, J., Thomson, A. J. and Hatchikian, E. C. (1991) *J. Am. Chem. Soc.* **115**, 8948–8950
- Butt, J. N., Niles, J., Armstrong, F. A., Breton, J. and Thomson, A. J. (1994) *Nat. Struct. Biol.* **1**, 427–433
- Butt, J. N., Fawcett, S. E. J., Breton, J., Thomson, A. J. and Armstrong, F. A. (1997) *J. Am. Chem. Soc.* **119**, 9729–9737
- Beinert, H., Kennedy, M. C. and Stout, C. D. (1996) *Chem. Rev.* **96**, 2335–2373
- Tong, J. and Feinberg, B. A. (1994) *J. Biol. Chem.* **269**, 24920–24927
- Staples, C. R., Dhawan, I. K., Finnegan, M. G., Dwinell, D. A., Zhou, Z. H., Huang, H., Verhagen, M. F. J. M., Adams, M. W. W. and Johnson, M. K. (1997) *Inorg. Chem.* **36**, 5740–5749
- Zhou, J., Raebiger, J. W., Crawford, C. A. and Holm, R. H. (1997) *J. Am. Chem. Soc.* **119**, 6242–6250
- George, S. J., Richards, A. J. M., Thomson, A. J. and Yates, M. G. (1984) *Biochem. J.* **224**, 247–251
- Armstrong, F. A., George, S. J., Thomson, A. J. and Yates, M. G. (1988) *FEBS Lett.* **234**, 107–111
- Johnson, M. K., Bennett, D. E., Fee, J. A. and Sweeney, W. V. (1987) *Biochim. Biophys. Acta* **911**, 81–94
- Shen, B., Martin, L. L., Butt, J. N., Armstrong, F. A., Stout, C. D., Jensen, G. M., Stephens, P. J., LaMar, G. N., Gorst, C. M. and Burgess, B. K. (1993) *J. Biol. Chem.* **268**, 25928–25939
- Hu, Z., Jollie, D., Burgess, B. K., Stephens, P. J. and Münck, E. (1994) *Biochemistry* **33**, 14475–14485
- Breton, J. L., Duff, J. L. C., Butt, J. N., Armstrong, F. A., George, S. J., Pétillot, Y., Forest, E., Schäfer, G. and Thomson, A. J. (1995) *Eur. J. Biochem.* **233**, 937–946
- Duff, J. L. C., Breton, J. L. J., Butt, J. N., Armstrong, F. A. and Thomson, A. J. (1996) *J. Am. Chem. Soc.* **118**, 8593–8603
- Beinert, H. and Kiley, P. (1996) *FEBS Lett.* **382**, 218–219
- Peters, J. W., Stowell, M. H. B., Soltis, S. M., Finnegan, M. G., Johnson, M. K. and Rees, D. C. (1997) *Biochemistry* **36**, 1181–1187
- Burgess, B. K. and Lowe, D. J. (1996) *Chem. Rev.* **96**, 2983–3011
- Aono, S., Bryant, F. O. and Adams, M. W. W. (1989) *J. Bacteriol.* **171**, 3433–3439
- Calzolari, L., Gorst, C. M., Zhao, Z.-H., Teng, Q., Adams, M. W. W. and LaMar, G. N. (1995) *Biochemistry* **34**, 11373–11384
- Gorst, C. M., Yeh, Y.-H., Teng, Q., Calzolari, L., Zhou, Z. H., Adams, M. W. W. and LaMar, G. N. (1995) *Biochemistry* **34**, 600–610
- Armstrong, F. A., George, S. J., Cammack, R., Hatchikian, E. C. and Thomson, A. J. (1989) *Biochem. J.* **264**, 265–273
- Busch, J. L. H., Breton, J. L., Bartlett, B. M., Armstrong, F. A., James, R. and Thomson, A. J. (1997) *Biochem. J.* **323**, 95–102
- Butt, J. N., Sucheta, A., Armstrong, F. A., Breton, J., Thomson, A. J. and Hatchikian, E. C. (1993) *J. Am. Chem. Soc.* **115**, 1413–1421
- Conover, R. C., Park, J.-B., Adams, M. W. W. and Johnson, M. K. (1991) *J. Am. Chem. Soc.* **113**, 2799–2800
- Telsler, J., Smith, E. T., Adams, M. W. W., Conover, R. C., Johnson, M. K. and Hoffman, B. M. (1995) *J. Am. Chem. Soc.* **117**, 5133–5140
- Zhou, Z. H. and Adams, M. W. W. (1997) *Biochemistry* **36**, 10892–10900
- Gorst, C. M., Zhou, Z. H., Ma, K., Teng, Q., Howard, J. B., Adams, M. W. W. and LaMar, G. N. (1995) *Biochemistry* **34**, 8788–8795
- Armstrong, F. A. (1997) *Bioelectrochemistry of Biomacromolecules*, vol. 5, pp. 205–255, Birkhäuser, Basel
- Hearing, H. A., Hirst, J. and Armstrong, F. A. (1997) *Chem. Soc. Rev.* **26**, 169–179
- Raven, N. D. H., Ladwa, N. M., Cossar, J. D. and Sharp, R. (1992) *Appl. Microbiol. Biotechnol.* **38**, 263–267
- Riddles, P. W., Blakeley, R. L. and Zerner, B. (1983) *Methods Enzymol.* **91**, 49–60
- Hirst, J., Duff, J. L. C., Jameson, G. N. L., Kemper, M. A., Burgess, B. K. and Armstrong, F. A. (1998) *J. Am. Chem. Soc.* **120**, 7085–7094
- Bard, A. J. and Faulkner, L. R. (1980) *Electrochemical Methods; Fundamentals and Applications*, Wiley, New York
- Thomson, A. J., Cheesman, M. R. and George, S. J. (1993) *Methods Enzymol.* **226**, 199–231
- Smith, E. T., Blamey, J. M., Zhou, Z. H. and Adams, M. W. W. (1995) *Biochemistry* **34**, 7161–7169
- Clark, W. M. (1961) *Oxidation-Reduction Potentials of Organic Systems*, Williams and Wilkins, Baltimore
- Thomson, A. J., Robinson, A. E., Johnson, M. K., Moura, J. J. G., Moura, I., Xavier, A. E. and LeGall, J. (1981) *Biochim. Biophys. Acta* **670**, 93–100
- Wilkins, R. G. (1991) *Kinetics and Mechanism of Reaction of Transition Metal Complexes*, 2nd edn., p. 16, VCH, Weinheim
- Fersht, A. (1985) *Enzyme Structure and Mechanism*, 2nd edn., p. 156, W. H. Freeman and Company, New York
- Bian, S., Hemann, C. F., Hille, R. and Cowan, J. A. (1996) *Biochemistry* **35**, 14544–14552
- Armstrong, F. A., Hill, H. A. O. and Walton, N. J. (1982) *FEBS Lett.* **150**, 214–218
- Roth, E. K. H. and Jordanov, J. (1992) *Inorg. Chem.* **31**, 240–243